Available online at www.sciencedirect.com
ScienceDirect
Journal of Computational and Applied Mathematics 214 (2008) 417–434
JOURNAL OF COMPUTATIONAL AND APPLIED MATHEMATICS
www.elsevier.com/locate/cam

Numerical solution of one-dimensional Burgers' equation using reproducing kernel function

Shu-Sen Xie[a,*,1], Sunyeong Heo[b], Seokchan Kim[c,2], Gyungsoo Woo[c], Sucheol Yi[c,3]

[a] *Department of Mathematics, Ocean University of China, Qingdao 266071, PR China*
[b] *Department of Statistics, Changwon National University, Changwon 641-773, Republic of Korea*
[c] *Department of Applied Mathematics, Changwon National University, Changwon 641-773, Republic of Korea*

Received 3 January 2006; received in revised form 12 February 2007

Abstract

This paper presents a numerical method for one-dimensional Burgers' equation by the Hopf–Cole transformation and a reproducing kernel function, abbreviated as RKF. The numerical solution is given as explicit integral expressions with the RKF at each time step, so that the computation is fully parallel. The stability and error estimates are derived. Numerical results for some test problems are presented and compared with the exact solutions. Some numerical results are also compared with the results obtained by other methods. The present method is easily implemented and effective.

MSC: 65M60; 65M99

Keywords: Burgers' equation; Hopf–Cole transformation; Reproducing kernel function

1. Introduction

Consider the one-dimensional quasi-linear Burgers' equation

$$\frac{\partial u}{\partial t} + u\frac{\partial u}{\partial x} = v\frac{\partial^2 u}{\partial x^2}, \tag{1}$$

where $v > 0$ is the coefficient of kinematic viscosity. Eq. (1) was first introduced by Bateman [2] and later treated by Burgers [4] after whom such an equation is widely referred to as Burgers' equation. This equation plays a major role in the study of nonlinear waves since it is used as a mathematical model in turbulence problems, in the theory of shock waves, and in continuous stochastic processes [5]. Many scientists are devoted to studying the exact and numerical

* Corresponding author.
E-mail addresses: shusenxie@ouc.edu.cn (S.-S. Xie), syheo@sarim.changwon.ac.kr (S. Heo), sckim@changwon.ac.kr (S. Kim), gswoo@changwon.ac.kr (G. Woo), scyi@changwon.ac.kr (S. Yi).

[1] The research of this author was supported by the National Natural Science Foundation of China (40276008).
[2] The research of this author was supported by the Korea Research Foundation Grant funded by the Korean Government (MOEHRD) (KRF-2002-070-C00014).
[3] The research of this author was supported by Changwon National University in 2005.

0377-0427/$ - see front matter © 2007 Elsevier B.V. All rights reserved.
doi:10.1016/j.cam.2007.03.010

solutions of this equation. Benton and Platzman [3] surveyed exact solutions of one-dimensional Burgers' equations. In many cases these solutions involve infinite series which may converge very slowly for small values of $\nu > 0$ [11]. Many other authors have used various numerical techniques to solve the equation numerically such as the techniques based on finite difference, finite element, boundary element, and spectral methods. (See [7–10,12,13], and literatures therein.)

In this paper, a numerical method will be formulated for solving Eq. (1) by applying the Hopf–Cole transformation [5] and a reproducing kernel function [1]. At each time step, the numerical solution is given explicitly by integral expressions of RKF even though the time discretization is implicit and, hence, the computation is fully parallel.

Let $\Omega = (a, b)$. Consider the following initial and boundary value problem:

$$\begin{aligned} &\frac{\partial u}{\partial t} + u\frac{\partial u}{\partial x} = \nu\frac{\partial^2 u}{\partial x^2}, \quad x \in \Omega, \ \ t \in (0, T], \\ &u(a, t) = u(b, t) = 0, \quad t \in (0, T], \\ &u(x, 0) = \phi(x), \quad x \in \Omega. \end{aligned} \tag{2}$$

Using the change of variable

$$u(x, t) = -2\nu\frac{\partial\theta/\partial x}{\theta}, \tag{3}$$

the nonlinear problem (2) can be reduced to the following linear initial and boundary value problem:

$$\begin{aligned} &\frac{\partial\theta}{\partial t} - \nu\frac{\partial^2\theta}{\partial x^2} = 0, \quad x \in \Omega, \ \ t \in (0, T], \\ &\frac{\partial\theta}{\partial x}(a, t) = \frac{\partial\theta}{\partial x}(b, t) = 0, \quad t \in (0, T], \\ &\theta(x, 0) = g(x), \quad x \in \Omega, \end{aligned} \tag{4}$$

where $g(x) = \exp(-(1/2\nu)\int_a^x \phi(s)\,\mathrm{d}s)$, which is known as the Hopf–Cole transformation. This means that if $\theta(x, t)$ is the solution of problem (4), then the solution of problem (2) is given by Eq. (3). The variational formulation of problem (4) is given as follows:

Find a function $\theta(\cdot, t) \mid (0, T] \to H^1(\Omega)$ such that

$$\begin{aligned} &\left(\frac{\partial\theta}{\partial t}, w\right) + \nu\left(\frac{\partial\theta}{\partial x}, \frac{\partial w}{\partial x}\right) = 0, \quad \forall w \in H^1(\Omega), \\ &\theta(x, 0) = g(x). \end{aligned} \tag{5}$$

Explicit iterative formulas for the numerical solution of problem (5) are formulated by an RKF in Section 2 and we discuss the stability and error estimates in Section 3. Finally, we present the numerical results obtained by the present method in Section 4.

2. Numerical solution

2.1. Semi-discrete approximation in time variable

Let τ denote the time step, $t^n = n\tau$, and let $\theta^n(x) = \theta(x, t^n)$ for $n = 0, 1, \ldots, T/\tau$. We proceed to discretize problem (5) first in the time variable t and consider the following discretized variational problem:

Find a function $\Theta^n \in H^1(\Omega)$ for $n = 1, 2, \ldots, T/\tau$ such that

$$\begin{aligned} &(\partial_t\Theta^n, w) + \nu\left(\beta\frac{\partial\Theta^n}{\partial x} + (1-\beta)\frac{\partial\Theta^{n-1}}{\partial x}, \frac{\partial w}{\partial x}\right) = 0, \quad \forall w \in H^1(\Omega), \\ &\Theta^0(x) = g(x), \end{aligned} \tag{6}$$

where $\partial_t\Theta^n = (\Theta^n - \Theta^{n-1})/\tau$ and β, $\frac{1}{2} \leqslant \beta \leqslant 1$, is a constant.

We will give the explicit expressions for the solution to semi-discrete problem (6) by using an RKF. Let $H(p, \Omega)$ denote the set of all functions in $H^1(\Omega)$ equipped with an inner product

$$\langle u,\ v\rangle = \int_\Omega \left(uv + p\frac{\mathrm{d}u}{\mathrm{d}x}\frac{\mathrm{d}v}{\mathrm{d}x}\right)\mathrm{d}x, \quad \forall u, v \in H(p, \Omega)$$

and a norm $|||\cdot||| = \sqrt{\langle\cdot,\cdot\rangle}$, where p is a positive constant. It is known that $H(p, \Omega)$ is a Hilbert space. For every $y \in \Omega$, we define a mapping $F_y : H(p, \Omega) \to R$ by

$$F_y(u) = u(y), \quad \forall u \in H(p, \Omega).$$

Then it can be easily seen that F_y is a bounded linear functional on $H(p, \Omega)$. Thus, it follows from Riesz's theorem that there exists a unique function $R_y \in H(p, \Omega)$ such that

$$u(y) = \langle u, R_y\rangle, \quad \forall u \in H(p, \Omega). \tag{7}$$

We call R_y satisfying Eq. (7) the RKF [1] of $H(p, \Omega)$.

Let

$$R(x, y) := R_y(x) = \frac{\cosh((b - \max(x, y))/\sqrt{p})\cosh((\min(x, y) - a)/\sqrt{p})}{\sqrt{p}\sinh((b - a)/\sqrt{p})}.$$

It is easy to verify that the function R_y is the RKF of $H(p, \Omega)$. By definition of the function R_y we have that

$$R(x, y) = R(y, x) > 0, \quad \forall x, y \in \Omega, \tag{8}$$

and it can be shown that the RKF $R_y \in H^1(\Omega)$ has the following properties (see [14]):

$$\int_a^b R(x, y)\,\mathrm{d}x = 1, \quad \forall y \in \Omega \tag{9}$$

and

$$\|u\|_{L_\infty(\Omega)} \leqslant \frac{\sqrt{\coth((b - a)/\sqrt{p})}}{\sqrt[4]{p}}|||u|||, \quad \forall u \in H(p, \Omega).$$

Let $p = \tau\nu\beta$. Then the first equation of problem (6) can be rewritten as

$$\langle\Theta^n, w\rangle = \frac{\beta - 1}{\beta}\langle\Theta^{n-1}, w\rangle + \frac{1}{\beta}(\Theta^{n-1}, w), \quad \forall w \in H(p, \Omega), \tag{10}$$

where $\langle\cdot,\cdot\rangle$ is the inner product on $H(p, \Omega)$. Setting $w = R_y$ in Eq. (10) we obtain

$$\Theta^n(x) = \frac{\beta - 1}{\beta}\Theta^{n-1}(x) + \frac{1}{\beta}\int_a^b \Theta^{n-1}(y)R(x, y)\,\mathrm{d}y, \quad \forall x \in \Omega \tag{11}$$

and

$$\frac{\partial\Theta^n}{\partial x}(x) = \frac{\beta - 1}{\beta}\frac{\partial\Theta^{n-1}}{\partial x}(x) + \frac{1}{\beta}\int_a^b \Theta^{n-1}(y)\frac{\partial R}{\partial x}(x, y)\,\mathrm{d}y, \quad \forall x \in \Omega. \tag{12}$$

By Eqs. (11), (12), and (3) we can obtain the time discrete approximation $U^n(x)$ to the solution of problem (2) given by

$$U^n(x) = -2\nu\frac{(\partial\Theta^n/\partial x)(x)}{\Theta^n(x)}, \quad n = 1, 2, \ldots, T/\tau.$$

2.2. Full-discrete approximation

Suppose that M_h is a finite element subspace of $H^1(\Omega)$ based on a family of subdivision with parameter h. Then each function w in M_h can be written in the form of

$$w(x) = \sum_{i=1}^{J} \mathcal{N}_i(w)\psi_i(x),$$

where $\mathcal{N}_i(w)$ is either the value or derivative of w at the ith node and the set $\{\psi_i\}_{i=1}^{J}$ is a basis for the space M_h.

If we choose $\Theta_h^0 = \mathcal{I}_h g$, where $\mathcal{I}_h$ is the interpolation operator onto M_h, then the full-discrete approximation of problem (4) is defined as follows:

Find a function $\Theta_h^n \in M_h$ for $n = 1, 2, \ldots, T/\tau$ such that

$$\Theta_h^n(x) = \frac{\beta - 1}{\beta}\Theta_h^{n-1}(x) + \frac{1}{\beta}\int_a^b \Theta_h^{n-1}(y)R(x, y)\,\mathrm{d}y. \tag{13}$$

Then we have

$$\begin{aligned}\Theta_h^n(x) &= \frac{\beta - 1}{\beta}\Theta_h^{n-1}(x) + \frac{1}{\beta}\sum_{i=1}^{J}\mathcal{N}_i(\Theta_h^{n-1})\int_a^b \psi_i(y)R(x, y)\,\mathrm{d}y \\ &= \frac{\beta - 1}{\beta}\Theta_h^{n-1}(x) + \frac{\cosh((b-x)/\sqrt{p})}{\beta\sqrt{p}\sinh((b-a)/\sqrt{p})}\sum_{i=1}^{J}\mathcal{N}_i(\Theta_h^{n-1})\Psi_{1,i}(x) \\ &\quad + \frac{\cosh((x-a)/\sqrt{p})}{\beta\sqrt{p}\sinh((b-a)/\sqrt{p})}\sum_{i=1}^{J}\mathcal{N}_i(\Theta_h^{n-1})\Psi_{2,i}(x), \quad \forall x \in \Omega,\end{aligned} \tag{14}$$

where

$$\Psi_{1,i}(x) = \int_a^x \psi_i(y)\cosh\frac{y-a}{\sqrt{p}}\,\mathrm{d}y \quad \text{and} \quad \Psi_{2,i}(x) = \int_x^b \psi_i(y)\cosh\frac{b-y}{\sqrt{p}}\,\mathrm{d}y.$$

The derivative of Θ_h^n at x is then given by

$$\begin{aligned}\frac{\partial\Theta_h^n}{\partial x}(x) &= \frac{\beta - 1}{\beta}\frac{\partial\Theta_h^{n-1}}{\partial x}(x) + \frac{1}{\beta}\int_a^b \Theta_h^{n-1}(y)\frac{\partial R}{\partial x}(x, y)\,\mathrm{d}y \\ &= \frac{\beta - 1}{\beta}\frac{\partial\Theta_h^{n-1}}{\partial x}(x) - \frac{\sinh((b-x)/\sqrt{p})}{\beta p\sinh((b-a)/\sqrt{p})}\sum_{i=1}^{J}\mathcal{N}_i(\Theta_h^{n-1})\Psi_{1,i}(x) \\ &\quad + \frac{\sinh((x-a)/\sqrt{p})}{\beta p\sinh((b-a)/\sqrt{p})}\sum_{i=1}^{J}\mathcal{N}_i(\Theta_h^{n-1})\Psi_{2,i}(x), \quad \forall x \in \Omega.\end{aligned} \tag{15}$$

By Eqs. (14), (15), and (3) we get the full-discrete approximation $U_h^n(x)$ to the solution of problem (2) given by

$$U_h^n(x) = -2v\frac{(\partial\Theta_h^n/\partial x)(x)}{\Theta_h^n(x)}, \quad n = 1, 2, \ldots, T/\tau.$$

We remark that expressions that are needed for the full-discrete approximation to the solution of problem (2) are given explicitly and are easy to evaluate.

3. Error and stability analysis

Throughout this paper, the symbol C denotes a generic positive constant, not necessarily the same at different occurrences. Let $\|\cdot\|_{W_q^m(\Omega)}$ denote the norm of Sobolev space $W_q^m(\Omega)$. The norm of $H^s(\Omega)$ is denoted by $\|\cdot\|_s$ and we write $\|\cdot\|_s$ as $\|\cdot\|$ when $s=0$. We assume that the finite element space M_h satisfies the following approximation property:

$$\min_{v\in M_h}\|w-v\|_{L_\infty(\Omega)}\leqslant Ch^r\|w\|_{W_\infty^r(\Omega)},\quad \forall w\in W_\infty^r(\Omega). \tag{16}$$

Let $f_\beta^n=\beta f^n+(1-\beta)f^{n-1}$ and $t_\beta^n=(n-1)\tau+\beta\tau$.

Theorem 1. *Suppose that* $\frac{1}{2}<\beta\leqslant 1$, θ *and* Θ^n *are the solutions of problems* (4) *and* (6), *respectively. If* $\Theta^0=g(x)\in H^1(\Omega)$, $\partial^2\theta/\partial t^2\in L_2(0,T;L_2(\Omega))$, *and* $\partial\theta/\partial t\in L_2(0,T;H^2(\Omega))$, *then we have*

$$\max_{1\leqslant n\leqslant T/\tau}\left\{\|\theta^n-\Theta^n\|^2+\nu\left\|\frac{\partial\theta^n}{\partial x}-\frac{\partial\Theta^n}{\partial x}\right\|^2\right\}\leqslant C\tau^2\int_0^T\left\{\left\|\frac{\partial^3\theta}{\partial x^2\partial t}\right\|^2+\left\|\frac{\partial^2\theta}{\partial t^2}\right\|^2\right\}\mathrm{d}t.$$

Proof. Let $\eta^n=\theta^n-\Theta^n$. From Eqs. (5) and (6), we can obtain the error equation

$$(\partial_t\eta^n,w)+\nu\left(\frac{\partial\eta_\beta^n}{\partial x},\frac{\partial w}{\partial x}\right)=\left(\partial_t\theta^n-\frac{\partial\theta}{\partial t}(t_\beta^n),w\right)-\nu\left(\frac{\partial^2\theta_\beta^n}{\partial x^2}-\frac{\partial^2\theta}{\partial x^2}(t_\beta^n),w\right). \tag{17}$$

Multiplying both the sides of Eq. (17) by τ with the function $w=\eta_\beta^n$, we obtain

$$\begin{aligned}&\frac{1}{2}(\|\eta^n\|-\|\eta^{n-1}\|)(\|\eta^n\|+\|\eta^{n-1}\|)+\left(\beta-\frac{1}{2}\right)\|\eta^n-\eta^{n-1}\|^2+\nu\left\|\frac{\partial\eta_\beta^n}{\partial x}\right\|^2\tau\\&\quad=\left(\partial_t\theta^n-\frac{\partial\theta}{\partial t}(t_\beta^n),\eta_\beta^n\right)\tau-\nu\left(\frac{\partial^2\theta_\beta^n}{\partial x^2}-\frac{\partial^2\theta}{\partial x^2}(t_\beta^n),\eta_\beta^n\right)\tau\\&\quad\leqslant\left\|\partial_t\theta^n-\frac{\partial\theta}{\partial t}(t_\beta^n)\right\|(\|\eta^n\|+\|\eta^{n-1}\|)\tau+\nu\left\|\frac{\partial^2\theta_\beta^n}{\partial x^2}-\frac{\partial^2\theta}{\partial x^2}(t_\beta^n)\right\|(\|\eta^n\|+\|\eta^{n-1}\|)\tau.\end{aligned}$$

Since $\frac{1}{2}<\beta$, we have

$$\begin{aligned}\|\eta^n\|-\|\eta^{n-1}\|&\leqslant 2\left\|\partial_t\theta^n-\frac{\partial\theta}{\partial t}(t_\beta^n)\right\|\tau+2\nu\left\|\frac{\partial^2\theta_\beta^n}{\partial x^2}-\frac{\partial^2\theta}{\partial x^2}(t_\beta^n)\right\|\tau\\&\leqslant C\tau\int_{t^{n-1}}^{t^n}\left\|\frac{\partial^2\theta}{\partial t^2}\right\|\mathrm{d}t+C\tau\int_{t^{n-1}}^{t^n}\left\|\frac{\partial^3\theta}{\partial x^2\partial t}\right\|\mathrm{d}t.\end{aligned}$$

If we replace n by k in the above inequality and sum on k from 1 to n, then we have

$$\|\eta^n\|\leqslant C\tau\int_0^{t^n}\left\|\frac{\partial^2\theta}{\partial t^2}\right\|\mathrm{d}t+C\tau\int_0^{t^n}\left\|\frac{\partial^3\theta}{\partial x^2\partial t}\right\|\mathrm{d}t$$

because $\eta^0 = 0$. Using the Cauchy inequality, we have

$$\|\eta^n\|^2 \leqslant C\tau^2 \int_0^{t^n} \left\{ \left\| \frac{\partial^2 \theta}{\partial t^2} \right\|^2 + \left\| \frac{\partial^3 \theta}{\partial x^2 \partial t} \right\|^2 \right\} \mathrm{d}t. \tag{18}$$

Taking $w = \partial_t \eta^n \tau$ in the error equation (17), we get

$$\begin{aligned} &\|\partial_t \eta^n\|^2 \tau + \frac{\nu}{2} \left(\left\| \frac{\partial \eta^n}{\partial x} \right\|^2 - \left\| \frac{\partial \eta^{n-1}}{\partial x} \right\|^2 \right) + \nu \left(\beta - \frac{1}{2} \right) \left\| \frac{\partial \eta^n}{\partial x} - \frac{\partial \eta^{n-1}}{\partial x} \right\|^2 \\ &\quad = \left(\partial_t \theta^n - \frac{\partial \theta}{\partial t}(t_\beta^n), \partial_t \eta^n \right) \tau - \nu \left(\frac{\partial^2 \theta_\beta^n}{\partial x^2} - \frac{\partial^2 \theta}{\partial x^2}(t_\beta^n), \partial_t \eta^n \right) \tau \\ &\quad \leqslant \frac{1}{2} \left\| \partial_t \theta^n - \frac{\partial \theta}{\partial t}(t_\beta^n) \right\|^2 \tau + \frac{\nu^2}{2} \left\| \frac{\partial^2 \theta_\beta^n}{\partial x^2} - \frac{\partial^2 \theta}{\partial x^2}(t_\beta^n) \right\|^2 \tau + \|\partial_t \eta^n\|^2 \tau. \end{aligned}$$

Then we obtain

$$\nu \left(\left\| \frac{\partial \eta^n}{\partial x} \right\|^2 - \left\| \frac{\partial \eta^{n-1}}{\partial x} \right\|^2 \right) \leqslant \left\| \partial_t \theta^n - \frac{\partial \theta}{\partial t}(t_\beta^n) \right\|^2 \tau + \nu^2 \left\| \frac{\partial^2 \theta_\beta^n}{\partial x^2} - \frac{\partial^2 \theta}{\partial x^2}(t_\beta^n) \right\|^2 \tau,$$

which implies that

$$\begin{aligned} \nu \left\| \frac{\partial \eta^n}{\partial x} \right\|^2 &\leqslant \sum_{k=1}^n \left\| \partial_t \theta^k - \frac{\partial \theta}{\partial t}(t_\beta^k) \right\|^2 \tau + \nu^2 \sum_{k=1}^n \left\| \frac{\partial^2 \theta_\beta^k}{\partial x^2} - \frac{\partial^2 \theta}{\partial x^2}(t_\beta^k) \right\|^2 \tau \\ &\leqslant C\tau^2 \int_0^{t^n} \left\{ \left\| \frac{\partial^2 \theta}{\partial t^2} \right\|^2 + \left\| \frac{\partial^3 \theta}{\partial x^2 \partial t} \right\|^2 \right\} \mathrm{d}t. \end{aligned} \tag{19}$$

Therefore, the result we wanted follows from inequalities (18) and (19). □

If $\beta = \frac{1}{2}$, then we have that

$$\sum_{k=1}^n \left\| \partial_t \theta^k - \frac{\partial \theta}{\partial t}(t_\beta^k) \right\| \tau \leqslant C\tau^2 \int_0^{t^n} \left\| \frac{\partial^3 \theta}{\partial t^3} \right\| \mathrm{d}t \tag{20}$$

and

$$\sum_{k=1}^n \left\| \frac{\partial^2 \theta_\beta^k}{\partial x^2} - \frac{\partial^2 \theta}{\partial x^2}(t_\beta^k) \right\| \tau \leqslant C\tau^2 \int_0^{t^n} \left\| \frac{\partial^4 \theta}{\partial x^2 \partial t^2} \right\| \mathrm{d}t. \tag{21}$$

Using inequalities (20) and (21), it can be seen that the following result holds by a similar argument as above.

Theorem 2. *Suppose that $\beta = \frac{1}{2}$, θ and Θ^n are the solutions of problems* (4) *and* (6), *respectively. If $\Theta^0 = g(x) \in H^1(\Omega)$, $\partial^3 \theta / \partial t^3 \in L_2(0, T; L_2(\Omega))$, and $\partial^2 \theta / \partial t^2 \in L_2(0, T; H^2(\Omega))$, then we have*

$$\max_{1 \leqslant n \leqslant T/\tau} \left\{ \|\theta^n - \Theta^n\|^2 + \nu \left\| \frac{\partial \theta^n}{\partial x} - \frac{\partial \Theta^n}{\partial x} \right\|^2 \right\} \leqslant C\tau^4 \int_0^T \left\{ \left\| \frac{\partial^4 \theta}{\partial x^2 \partial t^2} \right\|^2 + \left\| \frac{\partial^3 \theta}{\partial t^3} \right\|^2 \right\} \mathrm{d}t.$$

Taking $w = \Theta_\beta^n$ (or $w = \partial_t \Theta^n \tau$) in the first equation of problem (6) and using the same technique as above, we can obtain the following stability estimates.

Corollary 3. *Let Θ^n be the solution of problem* (6). *Then we have*

$$\|\Theta^n\| \leqslant \|\Theta^{n-1}\| \quad \textit{and} \quad \left\|\frac{\partial \Theta^n}{\partial x}\right\| \leqslant \left\|\frac{\partial \Theta^{n-1}}{\partial x}\right\|.$$

Integrating Eqs. (11) and (13) over Ω and using property (9), we get the following result.

Theorem 4. *Let Θ^n and Θ_h^n be the solutions of problems* (6) *and* (13), *respectively. Then we have that*

$$\int_a^b \Theta^n(x)\,\mathrm{d}x = \int_a^b \Theta^0(x)\,\mathrm{d}x \quad \textit{and} \quad \int_a^b \Theta_h^n(x)\,\mathrm{d}x = \int_a^b \Theta_h^0(x)\,\mathrm{d}x.$$

Remark. It is easy to verify that the exact solution θ of problem (4) satisfies that

$$\|\theta^n\| \leqslant \|\theta^{n-1}\|, \quad \left\|\frac{\partial \theta^n}{\partial x}\right\| \leqslant \left\|\frac{\partial \theta^{n-1}}{\partial x}\right\|, \quad \text{and} \quad \int_a^b \theta^n(x)\,\mathrm{d}x = \int_a^b \theta^0(x)\,\mathrm{d}x.$$

Corollary 3 and Theorem 4 show that the approximate solutions satisfy the same monotonicity and mass conservation property as the exact solution.

If $\beta = 1$, it follows from (8) and Eqs. (9), (11), and (13) that

$$|\Theta^n(x)| \leqslant \|\Theta^{n-1}\|_{L_\infty(\Omega)} \int_a^b R(x, y)\,\mathrm{d}y = \|\Theta^{n-1}\|_{L_\infty(\Omega)}$$

and

$$|\Theta_h^n(x)| \leqslant \|\Theta_h^{n-1}\|_{L_\infty(\Omega)} \int_a^b R(x, y)\,\mathrm{d}y = \|\Theta_h^{n-1}\|_{L_\infty(\Omega)}.$$

Then the following result follows from the above inequalities.

Theorem 5. *Suppose that Θ^n and Θ_h^n are the solutions of problems* (6) *and* (13), *respectively. If $\beta = 1$, then we have that*

$$\|\Theta^n\|_{L_\infty(\Omega)} \leqslant \|\Theta^0\|_{L_\infty(\Omega)} \quad \textit{and} \quad \|\Theta_h^n\|_{L_\infty(\Omega)} \leqslant \|\Theta_h^0\|_{L_\infty(\Omega)}.$$

Theorem 6. *Suppose that θ and Θ^n are the solutions of problems* (4) *and* (6), *respectively. If $\beta = 1$, $\Theta^0 = g(x) \in H^1(\Omega)$, and $\partial^2\theta/\partial t^2 \in L_1(0, T; L_\infty(\Omega))$, then we have*

$$\max_{1 \leqslant n \leqslant T/\tau} \|\theta^n - \Theta^n\|_{L_\infty(\Omega)} \leqslant C\tau \int_0^T \left\|\frac{\partial^2 \theta}{\partial t^2}\right\|_{L_\infty(\Omega)} \mathrm{d}t.$$

Proof. Let $\eta^n = \theta^n - \Theta^n$. From Eqs. (5) and (11), we can obtain the error equation

$$\eta^n(x) = \int_a^b \eta^{n-1}(y) R(x, y)\,\mathrm{d}y + \tau \int_a^b \left(\partial_t \theta^n(y) - \frac{\partial \theta^n}{\partial t}(y)\right) R(x, y)\,\mathrm{d}y.$$

Then we have

$$\|\eta^n\|_{L_\infty(\Omega)} \leqslant \|\eta^{n-1}\|_{L_\infty(\Omega)} + \tau \left\|\partial_t \theta^n - \frac{\partial \theta^n}{\partial t}\right\|_{L_\infty(\Omega)} \leqslant \|\eta^{n-1}\|_{L_\infty(\Omega)} + C\tau \int_{t^{n-1}}^{t^n} \left\|\frac{\partial^2 \theta}{\partial t^2}\right\|_{L_\infty(\Omega)} \mathrm{d}t.$$

Then the result follows immediately. □

Table 1
Numerical and exact solutions for $\nu = 1$ at different times with $h = 0.001$, $\tau = 0.001$

x	t	Numerical		Exact
		$\beta = 1$	$\beta = \frac{1}{2}$	
0.1	0.1	0.110095	0.109519	0.109538
	0.2	0.042324	0.041915	0.041929
	0.4	0.006040	0.005923	0.005927
0.3	0.1	0.293346	0.291846	0.291896
	0.2	0.111670	0.110584	0.110622
	0.4	0.015832	0.015523	0.015534
0.5	0.1	0.373352	0.371513	0.371577
	0.2	0.139797	0.138425	0.138473
	0.4	0.019605	0.019222	0.019235
0.7	0.1	0.311326	0.309851	0.309905
	0.2	0.114564	0.113429	0.113469
	0.4	0.015890	0.015579	0.015590
0.9	0.1	0.121225	0.120666	0.120687
	0.2	0.044113	0.043673	0.043689
	0.4	0.006076	0.005957	0.005961

Table 2
Error norms for $\nu = 1$ at different times with $h = 0.001$, $\tau = 0.001$

β		t		
		0.1	0.2	0.4
$\frac{1}{2}$	$\|e\|_{L_2} \times 10^5$	4.56483	3.39538	0.94262
	$\|e\|_{L_\infty} \times 10^5$	6.45697	4.80322	1.33307
1	$\|e\|_{L_2} \times 10^3$	1.25456	0.93638	0.26126
	$\|e\|_{L_\infty} \times 10^3$	1.77520	1.32452	0.36948

A similar argument as above can show that the following result holds.

Theorem 7. *Suppose that θ and Θ_h^n are the solutions of* (4) *and* (13), *respectively. If $\beta = 1$, $g(x) \in W_\infty^r(\Omega)$, $\partial^2\theta/\partial t^2 \in L_1(0, T; L_\infty(\Omega))$, and M_h satisfies the approximation property* (16), *then we have*

$$\max_{1 \leqslant n \leqslant T/\tau} \|\theta^n - \Theta_h^n\|_{L_\infty(\Omega)} \leqslant Ch^r \|g\|_{W_\infty^r(\Omega)} + C\tau \int_0^T \left\| \frac{\partial^2 \theta}{\partial t^2} \right\|_{L_\infty(\Omega)} \mathrm{d}t.$$

4. Numerical results

In this section, we will consider three test problems to test the accuracy and efficiency of the present method.

Example 1. The first example we considered has the initial and boundary conditions (see [9])

$$u(x, 0) = \sin(\pi x), \quad 0 < x < 1$$

and

$$u(0, t) = u(1, t) = 0, \quad 0 < t.$$

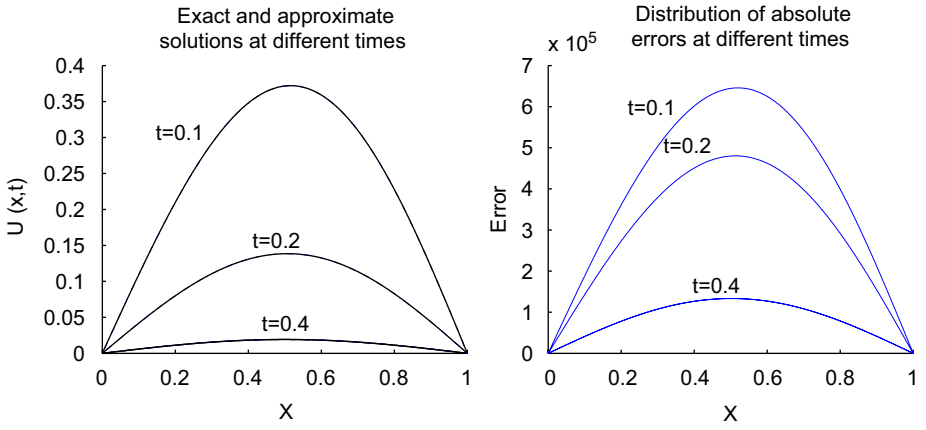

Fig. 1. Exact, numerical solutions (left), and distribution of absolute errors (right) for $v = 1$ at different times with $h = 0.001$, $\tau = 0.001$, and $\beta = \frac{1}{2}$.

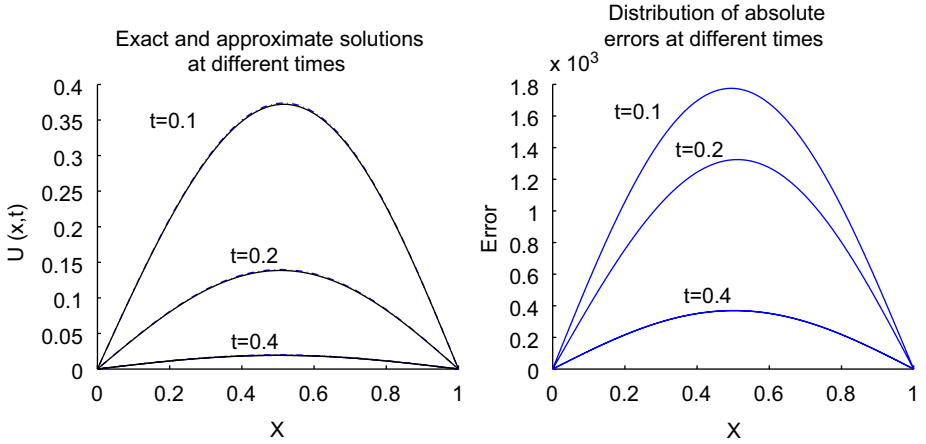

Fig. 2. Exact, numerical solutions (left), and distribution of absolute errors (right) for $v = 1$ at different times with $h = 0.001$, $\tau = 0.001$, and $\beta = 1$.

By the Hopf–Cole transformation the initial and boundary conditions to problem (4) are given by

$$\theta(x, 0) = \exp(-(2\pi v)^{-1}(1 - \cos(\pi x))), \quad 0 < x < 1$$

and

$$\frac{\partial \theta}{\partial x}(0, t) = \frac{\partial \theta}{\partial x}(1, t) = 0, \quad 0 < t.$$

In this case, the exact Fourier solution of problem (2) is given by

$$u(x, t) = 2\pi v \frac{\sum_{n=1}^{\infty} a_n \exp(-n^2\pi^2 v t) n \sin(n\pi x)}{a_0 + \sum_{n=1}^{\infty} a_n \exp(-n^2\pi^2 v t) \cos(n\pi x)}, \tag{22}$$

where

$$a_0 = \int_0^1 \exp(-(2\pi v)^{-1}(1 - \cos(\pi x))) \, \mathrm{d}x$$

Table 3
Numerical, exact solutions, and error norms for $v = 1$ at $t = 0.1$ with different step sizes $h = 0.025$, $\tau = 0.05$, and $\beta = \frac{1}{2}$

x	Numerical					Exact
	τ, h	$\frac{\tau}{2}, \frac{h}{2}$	$\frac{\tau}{4}, \frac{h}{4}$	$\frac{\tau}{8}, \frac{h}{8}$	$\frac{\tau}{16}, \frac{h}{16}$	
0.1	0.10668	0.10863	0.10928	0.10946	0.10951	0.10954
0.2	0.20422	0.20812	0.20932	0.20965	0.20974	0.20979
0.3	0.28408	0.28970	0.29127	0.29170	0.29183	0.29190
0.4	0.33880	0.34552	0.34724	0.34771	0.34785	0.34792
0.5	0.36244	0.36926	0.37091	0.37136	0.37150	0.37158
0.6	0.35115	0.35705	0.35846	0.35885	0.35897	0.35905
0.7	0.30406	0.30838	0.30945	0.30975	0.30985	0.30991
0.8	0.22420	0.22681	0.22751	0.22771	0.22778	0.22782
0.9	0.11902	0.12019	0.12053	0.12063	0.12067	0.12069
$\|e\|_{L_2} \times 10^3$	6.16074	1.64870	0.47693	0.15257	0.05496	
$\|e\|_{L_\infty} \times 10^3$	9.30489	2.41371	0.69236	0.21903	0.07817	

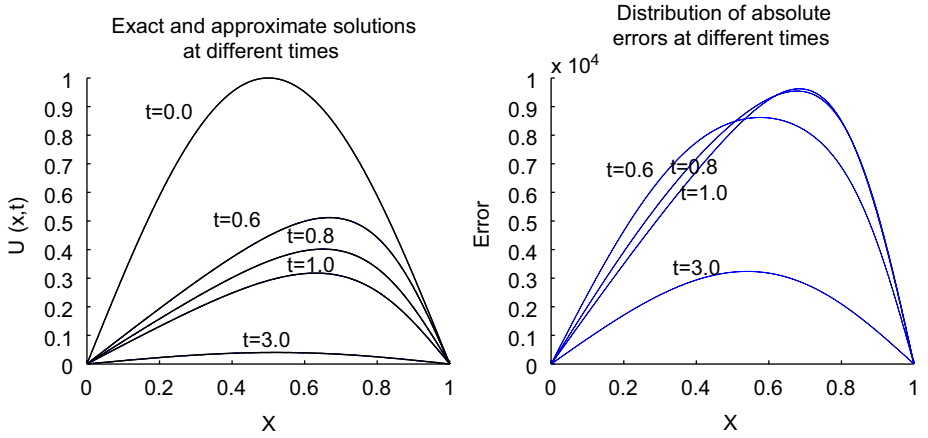

Fig. 3. Exact, numerical solutions (left), and distribution of absolute errors (right) for $v = 0.1$ at different times with $h = 0.00125$, $\tau = 0.01$, and $\beta = \frac{1}{2}$.

and

$$a_n = 2\int_0^1 \exp(-(2\pi v)^{-1}(1-\cos(\pi x)))\cos(n\pi x)\,\mathrm{d}x, \quad n = 1, 2, \ldots .$$

Example 2. As another example, we consider the Burgers' equation with initial condition

$$u(x, 0) = \sin(2\pi x), \quad 0 < x < 1$$

and boundary conditions

$$u(0, t) = u(1, t) = 0, \quad 0 < t.$$

This example is usually used for simulating the shock formation.

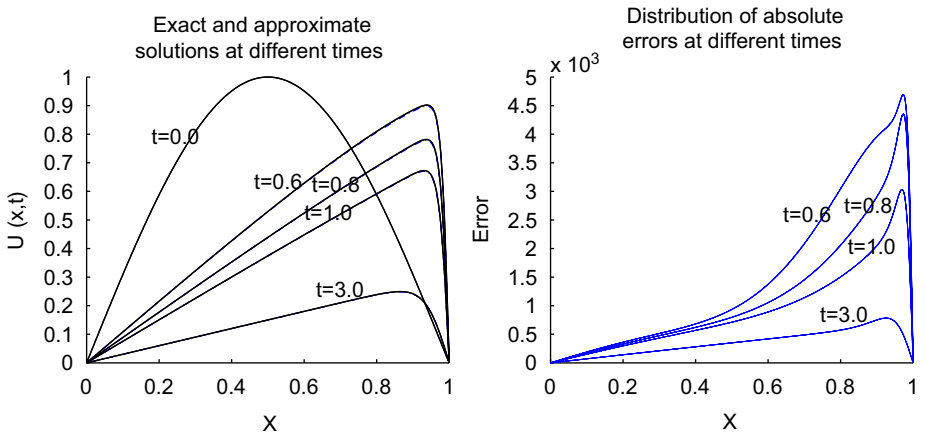

Fig. 4. Exact, numerical solutions (left), and distribution of absolute errors (right) for $v = 0.01$ at different times with $h = 0.00125$, $\tau = 0.01$, and $\beta = \frac{1}{2}$.

Table 4
Numerical, exact solutions for $v = 0.1$ and 0.01 at different times with $h = 0.00125$, $\tau = 0.01$, and $\beta = \frac{1}{2}$

x	t	$v = 0.1$		$v = 0.01$	
		Numerical	Exact	Numerical	Exact
0.25	0.4	0.30883	0.30889	0.34146	0.34191
	0.6	0.24068	0.24074	0.26853	0.26896
	0.8	0.19563	0.19568	0.22108	0.22148
	1.0	0.16252	0.16256	0.18783	0.18819
	3.0	0.02718	0.02720	0.07494	0.07511
0.50	0.4	0.56956	0.56963	0.65948	0.66071
	0.6	0.44712	0.44721	0.52848	0.52942
	0.8	0.35915	0.35924	0.43834	0.43914
	1.0	0.29183	0.29192	0.37371	0.37442
	3.0	0.04017	0.04021	0.14983	0.15018
0.75	0.4	0.62540	0.62544	0.90689	0.91026
	0.6	0.48714	0.48721	0.76470	0.76724
	0.8	0.37383	0.37392	0.64567	0.64740
	1.0	0.28738	0.28747	0.55475	0.55605
	3.0	0.02975	0.02977	0.22428	0.22481

By the Hope–Cole transformation, we have

$$\theta(x, 0) = \exp(-(4\pi v)^{-1}(1 - \cos(2\pi x))).$$

In this case, the exact Fourier solution is also given by Eq. (22), where

$$a_0 = \int_0^1 \exp(-(4\pi v)^{-1}(1 - \cos(2\pi x)))\,\mathrm{d}x$$

and

$$a_n = 2\int_0^1 \exp(-(4\pi v)^{-1}(1 - \cos(2\pi x)))\cos(n\pi x)\,\mathrm{d}x, \quad n = 1, 2, \ldots .$$

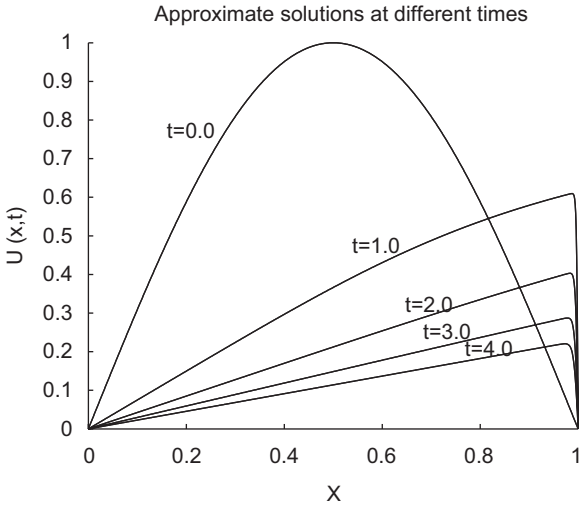

Fig. 5. Numerical solutions for $\nu = 0.001$ at different times with $h = 0.001$, $\tau = 0.01$, and $\beta = \frac{1}{2}$.

Table 5
Numerical, exact solutions, and error norms for $\nu = 1$ at $t = 0.1$ with different step sizes $h = 0.005$, $\tau = 0.01$, and $\beta = \frac{1}{2}$

x	Numerical					Exact
	τ, h	$\frac{\tau}{2}, \frac{h}{2}$	$\frac{\tau}{4}, \frac{h}{4}$	$\frac{\tau}{8}, \frac{h}{8}$	$\frac{\tau}{16}, \frac{h}{16}$	
0.1	0.01072	0.01116	0.01128	0.01131	0.01132	0.01132
0.2	0.01736	0.01808	0.01826	0.01831	0.01832	0.01833
0.3	0.01737	0.01809	0.01828	0.01833	0.01834	0.01835
0.4	0.01074	0.01119	0.01131	0.01134	0.01134	0.01135
0.5	0.00000	0.00000	0.00000	0.00000	0.00000	0.00000
0.6	−0.01074	−0.01119	−0.01131	−0.01134	−0.01134	−0.01135
0.7	−0.01737	−0.01809	−0.01828	−0.01833	−0.01834	−0.01835
0.8	−0.01736	−0.01808	−0.01826	−0.01831	−0.01832	−0.01833
0.9	−0.01072	−0.01116	−0.01128	−0.01131	−0.01132	−0.01132
$\|e\|_{L_2} \times 10^4$	7.23865	1.86939	0.49562	0.13794	0.04149	
$\|e\|_{L_\infty} \times 10^4$	10.23698	2.64370	0.70091	0.19508	0.05868	

Example 3. We considered the shock-like solution of the Burgers' equation. The exact analytic solution is given by (see [6,10])

$$u(x,t) = \frac{x/t}{1 + \sqrt{t/t_0}\exp(x^2/4\nu t)}, \quad t \geqslant 1, \tag{23}$$

where $t_0 = \exp(1/8\nu)$. The initial condition evaluated from (23) at time $t = 1$ is taken and boundary conditions $u(a,t) = u(b,t) = 0$ are used. By the Hopf–Cole transformation the initial and boundary conditions to problem (4) are given by

$$\theta(x,1) = \exp\left\{\log\left(\frac{1 + \sqrt{1/t_0}\exp(x^2/4\nu)}{1 + \sqrt{1/t_0}}\right) - \frac{x^2}{4\nu}\right\}, \quad a < x < b$$

and

$$\frac{\partial\theta}{\partial x}(a,t) = \frac{\partial\theta}{\partial x}(b,t) = 0, \quad 1 < t.$$

Most of our numerical experiments are done by using the finite element space M_h of piecewise linear functions.

Table 6
Numerical, exact solutions, and error norms for $\nu = 0.005$ at different times with $h = 0.001$, $\tau = 0.01$, and $\beta = \frac{1}{2}$

x	t					
	1.4		2.0		2.6	
	Numerical	Exact	Numerical	Exact	Numerical	Exact
0.1	0.06374	0.06394	0.04606	0.04621	0.03606	0.03618
0.2	0.12746	0.12784	0.09212	0.09241	0.07212	0.07234
0.3	0.19112	0.19168	0.13812	0.13854	0.10791	0.10826
0.4	0.25357	0.25434	0.17961	0.18022	0.13468	0.13521
0.5	0.00000	0.00000	0.00000	0.00000	0.00000	0.00000
0.6	−0.25357	−0.25434	−0.17961	−0.18022	−0.13468	−0.13521
0.7	−0.19112	−0.19168	−0.13812	−0.13854	−0.10791	−0.10826
0.8	−0.12746	−0.12784	−0.09212	−0.09241	−0.07212	−0.07234
0.9	−0.06374	−0.06394	−0.04606	−0.04621	−0.03606	−0.03618
$\|e\|_{L_2} \times 10^4$	5.54924		4.12911		3.30783	
$\|e\|_{L_\infty} \times 10^4$	10.85717		7.70085		6.00762	

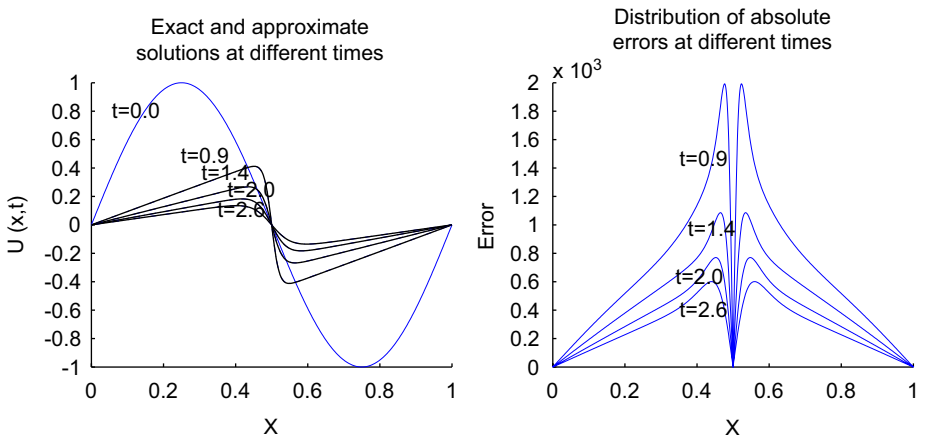

Fig. 6. Exact, numerical solutions (left), and distribution of absolute errors (right) for $\nu = 0.005$ at different times with $h = 0.001$, $\tau = 0.01$, and $\beta = \frac{1}{2}$.

Let $x_i = a + (i-1)h$, $h = (b-a)/(J-1)$ for $i = 1, 2, \ldots, J$. In this special case, the approximate solution has the form of

$$\Theta_h^n(x) = \sum_{i=1}^{J} \Theta_h^n(x_i)\psi_i(x),$$

where $\{\psi_i\}_{i=1}^J$ is a basis of the space M_h defined by

$$\psi_1(x) = \begin{cases} -(x - x_2)/h, & x \in [x_1, x_2], \\ 0 & \text{otherwise}, \end{cases}$$

$$\psi_J(x) = \begin{cases} (x - x_{J-1})/h, & x \in [x_{J-1}, x_J], \\ 0 & \text{otherwise}, \end{cases}$$

$$\psi_i(x) = \begin{cases} (x - x_{i-1})/h, & x \in [x_{i-1}, x_i], \\ -(x - x_{i+1})/h, & x \in [x_i, x_{i+1}], \\ 0 & \text{otherwise}. \end{cases} \quad i = 2, \ldots, J-1,$$

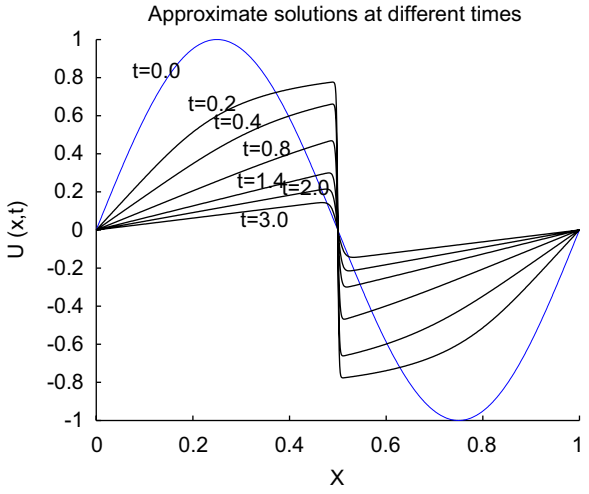

Fig. 7. Numerical solutions for $\nu = 0.001$ at different times with $h = 0.001$, $\tau = 0.01$, and $\beta = \frac{1}{2}$.

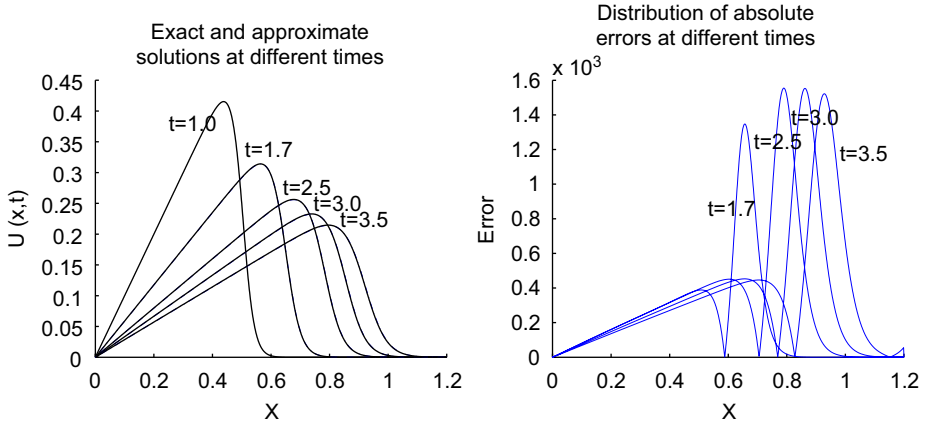

Fig. 8. Exact, numerical solutions (left), and distribution of absolute errors (right) for $\nu = 0.005$ at different times with $h = 0.001$, $\tau = 0.01$, and $\beta = \frac{1}{2}$.

The accuracy of our method will be measured using discrete L_2- and L_∞-error norms defined by

$$\|e^n\|_{L_2} = \left(\sum_{j=1}^{J} |e^n(x_j)|^2 h \right)^{1/2}, \quad \|e^n\|_{L_\infty} = \max_{1 \leqslant j \leqslant J} |e^n(x_j)|,$$

where $e^n(x_j) = u^n(x_j) - U_h^n(x_j)$.

Table 1 shows the numerical solutions of Example 1 for different values of β, say $\beta = \frac{1}{2}$ and 1. The numerical results for $\beta = \frac{1}{2}$ are better than those for $\beta = 1$ as we may expect. The errors in the discrete L_2- and L_∞-norms are given in Table 2. The numerical and corresponding exact solution curves are monitored in Figs. 1 and 2. The curves for distribution of absolute error at $t = 0.1$, 0.2, and 0.4 are also shown in Figs. 1 and 2. In these figures the exact (solid line) and numerical (dashdot line) solution curves are drawn in the left of each figure and they are in considerably good

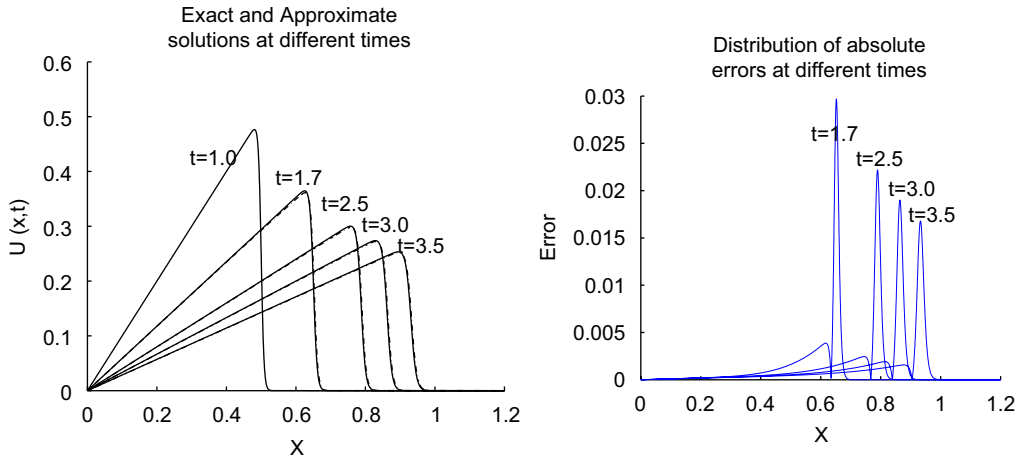

Fig. 9. Exact, numerical solutions (left), and distribution of absolute errors (right) for $\nu = 0.001$ at different times with $h = 0.0005$, $\tau = 0.01$, and $\beta = \frac{1}{2}$.

agreement. To test the rate of convergence, some numerical solutions and error norms computed by using different step sizes at $t = 0.1$ are presented in Table 3. One can see that the accuracy measured in the discrete L_2- and L_∞-norms increases monotonously as the step sizes get smaller. The rate of convergence is about 1.7 for both norms. Figs. 3 and 4 and Table 4 show a comparison between numerical and exact solutions for viscosity coefficients $\nu = 0.1$ and 0.01.

It is known that the Fourier solutions for $\nu < 0.01$ fail to converge because of the slow convergence of the infinite series (cf. [11]). The numerical solution curves for $\nu = 0.001$ at different times are drawn in Fig. 5, which shows the correct physical behavior. The curves in Fig. 5 are similar to the ones in [10].

The numerical experiments for Example 2 are done in the same pattern. The numerical solutions of Example 2, which are computed by using different step sizes at time $t = 0.1$, are given in Table 5. The accuracy measured in L_2- and L_∞-norms increases as the step sizes decrease. The numerical solutions are in the symmetric pattern as the exact solutions are. Table 6 and Fig. 6 show a comparison between numerical and exact solutions of Example 2 at different times for $\nu = 0.005$. The curves for distribution of absolute errors at different times are also shown in the right of Fig. 6. The numerical solutions at different times for $\nu = 0.001$ are drawn in Fig. 7, which shows the correct physical behavior. Fourier solutions do not converge for this small value of ν.

Example 3 is considered for the shock-like solution. In numerical experiments of Example 3, the exact, numerical solution, and absolute error distribution curves are given using different values of constants β, h, τ, and ν in Figs. 8 and 9. These figures show the stability of the present method and correct physical behavior. The numerical and exact solutions at different times are compared in Table 7 for the small value of $\nu = 0.005$ and Table 8 shows errors in discrete L_2- and L_∞-norms. In Table 9 the numerical and exact solutions are compared for the small value of $\nu = 0.001$ and the errors in discrete L_2- and L_∞-norms are also given. All numerical results obtained by the present method show good accuracies and agreements with exact solutions.

In order to test the effectiveness of higher degree basis functions, we considered numerical experiments for Example 1 with $\nu = 1$ at time $t = 0.1$ using piecewise quadratic polynomial basis functions. Numerical solutions and error norms obatined by using linear and quadratic basis functions are compared in Table 10. From Table 10 one can see that if quadratic basis functions were employed for the trial space M_h, a better accuracy can be obtained.

In numerical experiments of Example 3, we compared errors in discrete L_2- and L_∞-norms generated by using piecewise quadratic polynomial basis functions with the present method (the quadratic reproducing kernel function method, QRKM), the quadratic B-spline collocation method (QBCM, see [6]), the cubic B-spline collocation method (CBCM, see [6]), respectively. Table 11 shows that QRKM gives a better accuracy, which shows that the present method is effective and competitive.

Table 7
Numerical, exact solutions for $v = 0.005$ at different times with $h = 0.001$, $\tau = 0.01$, and interval $[a, b] = [0, 1.2]$

x	t	Numerical		Exact
		$\beta = 1$	$\beta = \frac{1}{2}$	
0.2	1.7	0.1176565	0.1174841	0.1176452
	2.5	0.0800527	0.0798389	0.0799990
	3.0	0.0667147	0.0665176	0.0666658
	3.5	0.0571820	0.0570060	0.0571422
0.4	1.7	0.2332111	0.2348504	0.2351677
	2.5	0.1591735	0.1596608	0.1599769
	3.0	0.1328314	0.1330273	0.1333209
	3.5	0.1139606	0.1140077	0.1142779
0.6	1.7	0.2940048	0.2961269	0.2959097
	2.5	0.2347876	0.2376699	0.2381207
	3.0	0.1973222	0.1990478	0.1994805
	3.5	0.1697753	0.1708231	0.1712242
0.8	1.7	0.0008917	0.0006640	0.0006465
	2.5	0.1103866	0.1036067	0.1020957
	3.0	0.2088346	0.2093735	0.2088359
	3.5	0.2119293	0.2143409	0.2145869

Table 8
Error norms for $v = 0.005$ at different times with $h = 0.001$, $\tau = 0.01$, and interval $[a, b] = [0, 1.2]$

β		t			
		1.7	2.5	3.0	3.5
$\frac{1}{2}$	$\|e\|_{L_2} \times 10^4$	3.84209	4.91345	5.15077	5.25855
	$\|e\|_{L_\infty} \times 10^4$	13.47279	15.54700	15.52891	15.21961
1	$\|e\|_{L_2} \times 10^3$	3.08966	2.72048	2.39922	2.12110
	$\|e\|_{L_\infty} \times 10^3$	10.40404	8.29747	6.98801	5.94321

Table 9
Numerical, exact solutions, and error norms for $v = 0.001$ at different times with $h = 0.0005$, $\tau = 0.01$, $\beta = \frac{1}{2}$, and interval $[a, b] = [0, 1.2]$

x	t					
	1.7		3.0		3.5	
	Numerical	Exact	Numerical	Exact	Numerical	Exact
0.2	0.11745	0.11765	0.06648	0.06667	0.05697	0.05714
0.4	0.23456	0.23529	0.13295	0.13333	0.11394	0.11429
0.6	0.34936	0.35291	0.19922	0.20000	0.17082	0.17143
0.8	0.00000	0.00000	0.26478	0.26662	0.22737	0.22857
1.0	0.00000	0.00000	0.00000	0.00000	0.000028	0.000020
$\|e\|_{L_2} \times 10^3$	3.59366		2.63510		2.41729	
$\|e\|_{L_\infty} \times 10^3$	29.70447		19.00976		16.78871	

Table 10
Numerical solutions of Example 1 using linear and quadratic polynomial basis for $\nu = 1$ at $t = 0.1$ with different step sizes $h = 0.025$, $\tau = 0.005$, and $\beta = \frac{1}{2}$

x	Numerical				Exact
	Linear		Quadratic		
	τ, h	$\frac{\tau}{2}, \frac{h}{2}$	τ, h	$\frac{\tau}{2}, \frac{h}{2}$	
0.1	0.10895	0.10925	0.10951	0.10953	0.10954
0.2	0.20866	0.20925	0.20973	0.20978	0.20979
0.3	0.29032	0.29113	0.29182	0.29188	0.29190
0.4	0.34603	0.34701	0.34784	0.34790	0.34792
0.5	0.36955	0.37059	0.37150	0.37156	0.37158
0.6	0.35708	0.35809	0.35898	0.35903	0.35905
0.7	0.30820	0.30907	0.309986	0.30989	0.30991
0.8	0.22656	0.22720	0.22779	0.22781	0.22782
0.9	0.12002	0.12036	0.12067	0.12068	0.12069
$\|e\|_{L_2} \times 10^3$	1.43560	0.69757	0.05407	0.01346	
$\|e\|_{L_\infty} \times 10^3$	2.03069	0.98711	0.08056	0.02006	

Table 11
Error norms for Example 3 using quadratic polynomial basis at different times with $\nu = 0.005$, $h = 0.005$, $\tau = 0.01$, $\beta = \frac{1}{2}$, and interval $[a, b] = [0, 1]$

		t		
		1.7	2.5	3.25
QRKM	$\|e\|_{L_2} \times 10^3$	0.02681	0.03135	1.11149
	$\|e\|_{L_\infty} \times 10^3$	0.09174	0.11515	8.00069
QBCM [6]	$\|e\|_{L_2} \times 10^3$	0.07215	0.05103	1.24901
	$\|e\|_{L_\infty} \times 10^3$	0.31153	0.18902	8.98390
CBCM [6]	$\|e\|_{L_2} \times 10^3$	2.46642	2.11187	1.92482
	$\|e\|_{L_\infty} \times 10^3$	27.5770	25.1517	21.0489

Acknowledgment

The authors would like to thank the anonymous referees for their valuable comments on this paper.

References

[1] Z. Aronszajn, Theory of reproducing kernels, Trans. Amer. Math. Soc. 68 (1950) 337–404.
[2] H. Bateman, Some recent researches on the motion of fluids, Monthly Weather Rev. 43 (1915) 163–170.
[3] E. Benton, G.W. Platzman, A table of solutions of the one-dimensional Burgers equations, Quart. Appl. Math. 30 (1972) 195–212.
[4] J.M. Burgers, A mathematical model illustrating the theory of turbulence, Adv. Appl. Mech. 1 (1948) 171–199.
[5] J.D. Cole, On a quasi-linear parabolic equation occurring in aerodynamics, Quart. Appl. Math. 9 (1951) 225–236.
[6] İ. Dağ, D. Irk, A. Sahin, B-spline collocation methods for numerical solutions of the Burgers equation, Math. Problems in Eng. 5 (2005) 521–538.
[7] C.A. Fletcher, A comparison of finite element and difference solutions of the one and two dimensional Burgers' equations, J. Comput. Phys. 51 (1983) 159–188.
[8] K. Kakuda, N. Tosaka, The generalized boundary element approach to Burgers' equation, Internat. J. Numer. Methods Eng. 29 (1990) 245–261.
[9] S. Kutluay, A.R. Bahadir, A. Özdes, Numerical solution of one-dimensional Burgers equation: explicit and exact-explicit finite difference methods, J. Comput. Appl. Math. 103 (1999) 251–261.
[10] S. Kutluay, A. Esen, İ. Dağ, Numerical solutions of the Burgers equation by the least-squares quadratic B-spline finite element method, J. Comput. Appl. Math. 167 (2004) 21–33.
[11] E.L. Miller, Predictor–corrector studies of Burgers' model of turbulent flow, M.S. Thesis, University of Delaware, Newark, DE, 1966.

[12] R.C. Mittal, P. Singhal, Numerical solution of Burgers' equation, Comm. Numer. Methods Eng. 9 (1993) 397–406.
[13] R.C. Mittal, P. Singhal, Numerical solution of periodic Burgers' equation, Indian J. Pure Appl. Math. 27 (1996) 689–700.
[14] S.-S. Xie, New numerical methods for some initial–boundary value problems and applications, Ph.D. Thesis, Shandong University, PR China, 1996.